

# A perspective on effective medium models of thermal conductivity in (ultra)nanocrystalline diamond films

Titus Sandu

*National Institute for Research and Development in Microtechnologies-IMT, 126A, Erou Iancu Nicolae Street, Bucharest, Romania*

Catalin Tibeica

*National Institute for Research and Development in Microtechnologies-IMT, 126A, Erou Iancu Nicolae Street, Bucharest, Romania*

---

## Abstract

Thermal conductivity of nanocrystalline and ultra-nanocrystalline films is analyzed with effective medium theory (EMT) models. The existing EMT models use the spherical inclusion approximation. Although this approximation works quite well it is inconsistent, mostly with respect to the maximal packing of 74%, which may be unrealistic for polycrystalline films. To check the consistency of these models we devise an EMT model with arbitrarily shaped inclusions. We pick the EMT model with cubic inclusions and we compare its results with the results of the EMT model with spherical inclusions. It is found a very good agreement between both calculations. This agreement is explained by general geometrical arguments. We further employ these models to analyze thermal conductivity of nanocrystalline and ultra-nanocrystalline diamond films. It is noticed that the effective conductivity is strongly affected not only by the boundary Kapitza resistance but also by intra-grain scattering for grain sizes below 100 nm. Generally, both intra-grain conductivity and Kapitza resistance increase with grain size. However, the effect of Kapitza resistance increase is negligible due to the geometrical factor accompanying Kapitza resistance contribution to the effective conductivity.

*Keywords:* thermal conductivity, coherent potential approximation, polycrystalline films, effective medium theory, nanocrystalline diamond, ultra-nanocrystalline diamond

---

## 1. Introduction

Thermal properties of nanocrystalline materials are of great interest in fields like micro/nanoelectromechanical systems (M/NEMS) or thermal management of electronics for thermal interface materials [1]. In particular, nanocrystalline materials like nanocrystalline diamond (NCD) and ultrananocrystalline diamond (UNCD) films are also ideal candidates for mechanical and electronic applications with outstanding properties [2].

The NCD films are defined as polycrystalline materials containing grains with sizes between tens of nm and 1  $\mu\text{m}$ , while the UNCD films contain grains having sizes between 2 to 10 nm [3]. On the other hand, the allotrope forms of carbon such as diamond, graphene, or nanotubes are the best ever known heat conductors, with their heat conductivity an order of magnitude larger than any metal [2]. In a bulk material thermal conductivity is given by the following equation obtained from a kinetic theory:  $\kappa=C_V V_g \Lambda/3$ .  $C_V$  is the heat capacity,  $V_g$  is the average phonon group velocity, and  $\Lambda$  is the phonon mean free path. However, thermal conductivity of nanocrystalline materials and of NCD and UNCD films, in particular, are considerably reduced due to grain boundary effects which add a boundary thermal resistance and reduced mean free paths of phonons from their bulk values [4, 5].

*Generally, thermal conductivity of nanocrystalline materials decreases with the decrease of crystallite size* [4, 5]. Microscopic techniques such as Boltzmann transport equation [6] and Monte Carlo simulations [7] can consider detailed phonon grain boundary scattering but they are numerically intensive and also expensive. Another microscopic approach is the phonon-hopping model [8]. The model assumes that in a nanograin the phonon transport is governed by the same mechanisms as in bulk crystal and introduces a phonon hopping parameter, which describes the phonon transport from one grain to the next one. Although the phonon-hopping model is able to predict the temperature dependence of the effective thermal conductivity [9], one can easily show that the model is equivalent to the effective medium theory (EMT) of Yang *et al.* [10]. Furthermore, even a combined serial/parallel heat conduction model like that used to explain thermal conductivity in NCD films [11] can be cast into the form given in [10].

The EMT model of Yang *et al.* is based on the EMT of Nan and Birringer, who considered spheres as shapes for crystallites [4]. However, the

maximal packing obtained with equally-sized spheres is 74%, therefore one may encounter some inconsistencies of the model based on spherical crystallites. In addition, spherical crystallites are inconsistent with the assumption of planar interfaces between grains made in the model described in ref. [10]. Moreover, in the EMT model of Yang *et al.* the grain conductivity is simply the bulk conductivity. This model can be further improved by adjusting the phonon mean free path of the grain to the grain size [8, 9]. Recently, Dong *et al.* refined the model of Yang *et al.* by considering an intra-grain conductivity that is different from the bulk value and is affected by the phonon scattering at the grain boundary [12].

In this work we analyze the effective thermal conductivity of nanocrystalline and ultra-nanocrystalline films with various EMT models. We relate our recent results regarding the homogenization of heterogeneous materials [13] to the EMT models expressed in Refs. [4, 8, 9]. We devise an EMT with arbitrarily shaped crystallites and we compare an EMT model with cubic-shaped crystallites in 3D and square-shaped crystallites in 2D with the model of Yang *et al.* [10]. We further analyze the influence of various factors like crystallite size, phonon scattering at the grain boundary, and boundary thermal resistance on the thermal conductivity of NCD and UNCD materials. Our paper is structured as follows. In the next section we present the effective medium models of thermal conductivity in polycrystalline materials and our results regarding the EMT model with arbitrarily shaped crystallites. In section 3 we present numerical results and our analysis regarding thermal conductivity of NCD and UNCD materials. The last section is dedicated to conclusions.

## **2. Effective Medium Models of thermal conductivity in nanocomposites and polycrystalline materials**

In the modeling of composites the electric, dielectric, or thermal phenomena can be treated similarly, since the governing equations are the same [14]. Moreover, if the composite has a granular structure (a collection of inclusions dispersed into a matrix), the calculations of the composite effective parameters can start from the behavior of a single inclusion embedded in the matrix. Having the response of a single inclusion and considering the interactions between inclusions, the effective parameters of the composite can be calculated with various degrees of accuracy [14]. This process may be called a homogenization process by which the response of a heterogeneous system is similar

to that of a homogeneous system characterized by the effective parameters calculated in the process. The response of a particle of volume  $V_1$  immersed in a uniform matrix and exposed to a uniform heat flux can be defined as [13]

$$\alpha = \frac{1}{4\pi V_1} \int_{V_1} \frac{(\kappa_1 - \kappa_0)}{\kappa_0} (-\nabla T(r)) d^3 r. \quad (1)$$

In Eq. (1)  $\kappa_1$  and  $\kappa_0$  are the conductivities of the particle and of the embedding medium, respectively and  $T$  is the temperature field calculated in the presence of the particle. In dielectric phenomena  $\alpha$  is the normalization polarizability which can be cast as in the following [13, 15]

$$\alpha = \sum_k \frac{w_k (\kappa_1 - \kappa_0)}{\kappa_0 + L_k (\kappa_1 - \kappa_0)}, \quad (2)$$

where  $L_k$  is the depolarization factor of the  $k^{th}$  eigenmode of an electrostatic operator defined on the boundary of  $V_1$  and  $w_k$  is the weight of this eigenmode. It can be readily seen that  $\alpha$  is related to the  $t$ -matrix formalism of the scattering theory [14, 16]. In addition, the interfacial barrier resistance between the inclusion and the matrix is modeled as a very thin shell of thermal conductivity  $\kappa_2$  [4, 10, 14]. The shelled particle can be also “homogenized” by simply replacing it with a similar particle, which has an effective conductivity for each eigenmode given by [13, 15]:

$$\kappa_{k-1} = \kappa_2 \left( 1 + \frac{\kappa_1 - \kappa_2}{(1 + \eta) \kappa_2 + \eta(1/2 - \chi_k) (\kappa_1 - \kappa_2)} \right), \quad (3)$$

where  $1 + \eta$  is a volume ratio between the particle with and without the shell. Equation (3) is a generalization of the results from [4, 17] to arbitrarily shaped nanoparticles. It is easy to check that interfacial resistance is obtained in the limit  $\eta \rightarrow 0$  and  $\eta/\kappa_2 \rightarrow \text{constant}$  as

$$\kappa_{k-1} = \frac{\kappa_1}{1 + d\kappa_1 L_k R_K / l}, \quad (4)$$

where  $d$  is the dimension of the problem, which is 3 for a 3D problem and 2 for a 2D problem,  $R_K$  is the Kapitza boundary resistance and  $l$  is a characteristic length of the particle. In Eq. (4) we considered that the grain boundary is shared between two adjacent grains as in the paper of Yang *et al.* [10].

Once the response of a single inclusion is calculated various procedures can be devised in order to obtain effective medium models. One of the oldest and the most successful effective medium models is the Maxwell-Garnett approximation, which is an averaged  $t$ -matrix approximation [14, 16]. The Maxwell-Garnett approximation works well for low volume concentrations of the filler [13]. For large volume concentrations, however, the coherent potential approximation (CPA) is more appropriate [13, 14].

In CPA, the effective conductivity  $\kappa_{eff}$  is obtained by setting the average of  $\alpha$  over the composite to zero, i. e.,  $\langle \alpha \rangle = 0$ . For arbitrarily-shaped inclusions the explicit form of CPA is [13]

$$\sum_k f \frac{w_k (\kappa_{k-1} - \kappa_{eff})}{\kappa_{eff} + L_k (\kappa_{k-1} - \kappa_{eff})} + (1 - f) \frac{w_k (\kappa_0 - \kappa_{eff})}{\kappa_{eff} + L_k (\kappa_0 - \kappa_{eff})} = 0, \quad (5)$$

where  $f$  is the volume concentration of the inclusions. When the inclusions with a boundary thermal resistance fill the whole composite, i. e.,  $f = 1$ , Eq. (5) becomes

$$\sum_k \frac{w_k (\kappa_{k-1} - \kappa_{eff})}{\kappa_{eff} + L_k (\kappa_{k-1} - \kappa_{eff})} = 0, \quad (6)$$

which can be a model for thermal conductivity of polycrystalline films and an extension of the model used by Nan for spherical and ellipsoidal grains [4]. A graphical illustration of EMT described by Eq. (6) is given in Fig. 1, where the grain with its boundary is transformed into a homogeneous body and then the process is applied to the whole material.

Generally, Eq. (6) has as many solutions as the number of eigenmodes present in the response. However, just one solution has physical significance, which must be a positive root. A practical way to evaluate the effective thermal conductivity  $\kappa_{eff}$  is to look for a solution that satisfies  $|\kappa_{k-1} - \kappa_{eff}| \ll \kappa_{eff}$ . Knowing that  $0 < L_k < 1$  and using the sum rule  $\sum_k w_k = 1$  [15, 18], the following approximation can be obtained

$$\kappa_{eff} = \sum_k \frac{w_k \kappa_1}{1 + d\kappa_1 L_k R_K / l}, \quad (7)$$

where  $\kappa_1$  is the grain thermal conductivity of the grain. In the case of spherical grain  $L_k = 1/3$  and  $w_k = 1$  thus Eqs. (6) and (7) have the form similar to that given in Ref. [10]

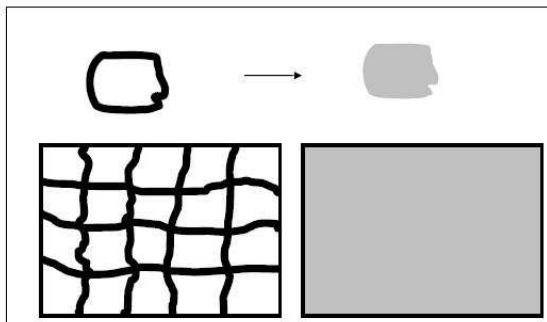


Figure 1: Process of homogenization in nanocrystalline materials. It is represented by the homogenization of a grain and its boundary (top), followed by the homogenization of the whole material. The thick black lines represent the grain boundaries.

$$\kappa_{eff3D} = \frac{\kappa_1}{1 + R_K \kappa_1 / l}, \quad (8)$$

where  $l$  is the diameter of the spherical grain. Eq. (8) considers that the inter-grain space is shared between two adjacent grains [10]. In the original work of Nan and Birringer (Ref. [4]), the diameter  $l$  was replaced by the sphere radius.

### 3. Thermal conductivity models of NCD and UNCD films. Discussion

#### 3.1. 3D models

The model of Nan and Birringer assumes spherical grains, but in reality the grains have polyhedral shapes and it is supposed that their departure from spherical shape is quite small. There are, at least, two major issues here regarding the effective medium models with spherical inclusions. The maximal packing of equal spheres is about 74%, while for randomly arranged spheres the packing is even smaller [19]. The second issue is about the argument of Yang *et al.* [10], who made the reasoning of interface thermal resistance for planar interfaces. Thus it is natural to ask if the shape averaging can be made around cubic rather than spherical shape. For cubic geometry the packing can reach 100% and cubic shape is also compatible with planar interfaces encountered in polycrystalline materials. In the following we compare the results provided by the effective medium model using

spherical inclusions with the effective medium model that assumes cubic inclusions. For cube we use the spectral parameters calculated in Ref. [18], namely  $w_1 = 0.44$ ,  $L_1 = 0.214$ ,  $w_2 = 0.24$ ,  $L_2 = 0.297$ ,  $w_3 = 0.04$ ,  $L_3 = 0.345$ ,  $w_4 = 0.05$ ,  $L_4 = 0.440$ ,  $w_5 = 0.01$ ,  $L_5 = 0.563$ ,  $w_6 = 0.09$ ,  $L_6 = 0.706$ ,  $w_7 = 0.04$ ,  $L_7 = 0.33$ . In the cubical model  $l$  is the edge length of the cube.

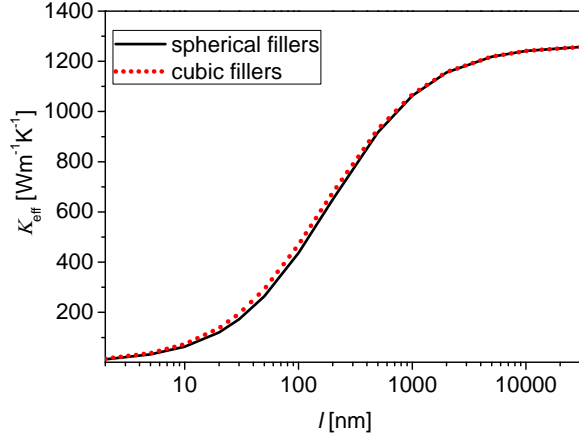


Figure 2: The effective thermal conductivities given by the EMT with spherical (solid black line) versus cubic (dotted red line) shaped crystallites.

In order to assess the effectiveness of Eq. (7) we compare its outcome with the results provided by the full form of Eq. (6) for polycrystalline diamond using the model with cubic inclusions. The results were apart by less than 1% for cubic inclusions of edge lengths ranging from 2 nm to 10  $\mu\text{m}$ , hence Eq. (7) provides reliable results. In Fig. 2 we compare the effective medium models of spherical (Eq. (7)) and cubic inclusions (Eq. (8)). The bulk thermal conductivity is  $1265 \text{ Wm}^{-1}\text{K}^{-1}$  taken from molecular dynamics simulations [12] and  $R_K = 1.0 \times 10^{-9} \text{ Km}^2/\text{W}$ . As we can see from Fig. 2 there is a very good match between the model with spherical inclusions and the model with cubic inclusions.

### 3.2. 2D models

In 2D the filling factor of the plane with circles is  $\pi/4 \approx 78.5\%$ . Moreover, for a two-dimensional model of a polycrystalline films with circular inclusions, Eqs (4) and (6) provide a similar formula to Eq. (8), i. e.,

$$\kappa_{eff2D} = \frac{\kappa_1}{1 + R_K \kappa_1 / l}, \quad (9)$$

where  $l$  is the diameter of the circle. We recall that in 2D the depolarization factor of a circle is  $L_k = 1/2$  [20].

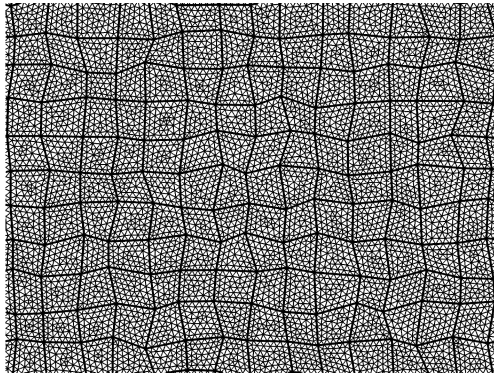


Figure 3: A FEM simulation box to calculate the effective thermal conductivity of a 2D polycrystalline material. Thick lines define the grain boundaries and thinner lines show the mesh.

To check the validity of Eq. (9) in 2D we performed finite element (FEM) calculations with the commercial software COMSOL. We started with a simulation box that was divided in equal-sized squares which are associated with the crystallites. Each crystallite exhibits an interface thermal resistance. To mimic the random variation about square shape of the crystallites we moved



each vertex by a random quantity between the values  $dx$  and  $-dx$  and between  $dy$  and  $-dy$  on  $x$ - and  $y$ -axes, respectively (for convenience we took  $dx = dy$ ). A sample of the simulation box is given in Fig. 3. The interface thermal resistance is depicted by thick separating lines. In calculations there were used the following values:  $R_K=1 \times 10^{-9}$   $\text{Km}^2/\text{W}$  for Kapitza interface resistance and  $\kappa=2200$   $\text{Wm}^{-1}\text{K}^{-1}$  for thermal conductivity.

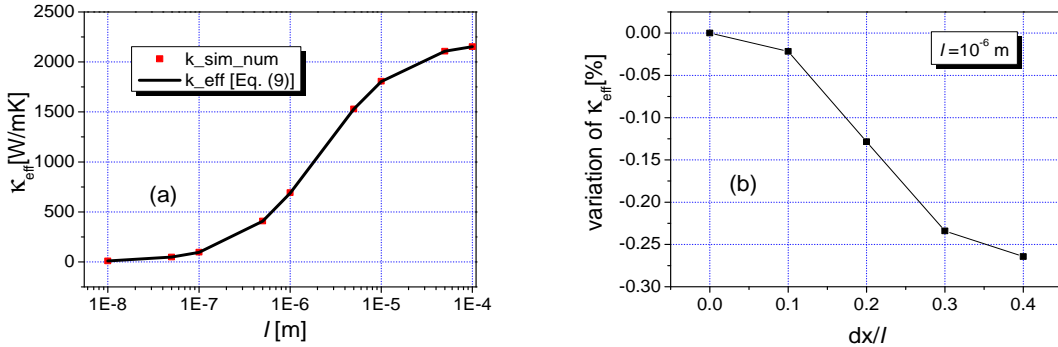


Figure 4: (a) Comparison between calculations with a FEM method and Eq. (9). The analytical results were plotted with solid black line, while the FEM results are illustrated by red square symbols; (b) The relative variation of thermal conductivity with respect to the size fluctuation  $dx$  in FEM calculations.

In Fig. 4(a) we compare the results of FEM calculations with Eq. (9) that gives the thermal conductivity of the EMT with circular inclusions. FEM calculations provide an averaging about square-shaped inclusions. Inspecting Fig. 4(a) we may conclude that results obtained by averaging about circular-shaped inclusions are similar to the results obtained by averaging around square-shaped inclusions. In Fig. 4(b) it is shown that variation of the results with respect to the size of  $dx$  is far less than 1%.

### 3.3. The effect of intra-grain conductivity on the effective conductivity of NCD and UNCD films

In Eqs. (7)-(9)  $\kappa_1$  is basically the bulk thermal conductivity, which cannot be the intra-grain conductivity at least for grains whose sizes are smaller than the bulk phonon mean free path. In many calculations the phonon mean free path is replaced by the actual size of the grain. However, recently Dong *et al.* found an intra-grain conductivity that includes basically all the intra-grain scattering events [12]. By molecular dynamics simulations the authors

obtained the intra-grain conductivity such that the final EMT formula for thermal conductivity in nanocrystalline materials is

$$\kappa_{eff} = \frac{\kappa_1/(1 + \Lambda/l^{0.75})}{1 + R_K [\kappa_1/(1 + \Lambda/l^{0.75})]/l}. \quad (10)$$

In Eq. (10)  $\kappa_{eff}$  and  $\kappa_1$  are given in  $\text{Wm}^{-1}\text{K}^{-1}$ , the bulk phonon mean free path  $\Lambda$  and the size of the grain  $l$  are given in nm, while  $R_K$  is provided in  $\text{m}^2\text{KW}^{-1}$ . Dong *et al.* calculated a diamond bulk thermal conductivity of  $1265 \text{ Wm}^{-1}\text{K}^{-1}$  and a diamond phonon mean free path  $\Lambda$  of 180 nm.

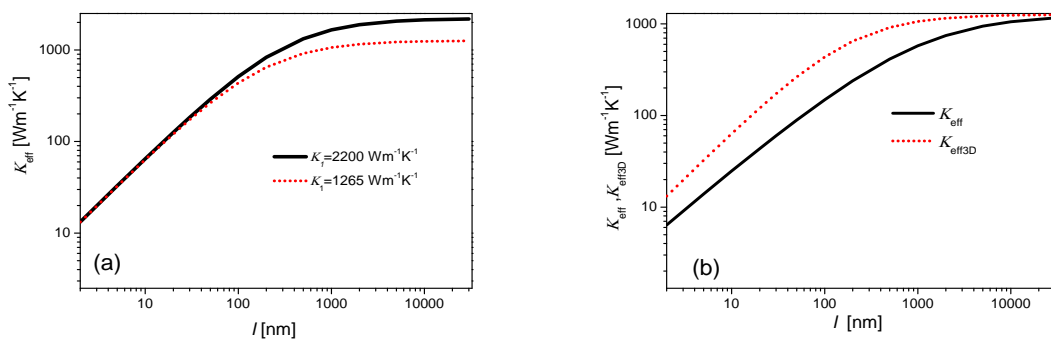


Figure 5: (a) The effect of the bulk thermal conductivity on the effective conductivity of NCD and UNCD materials modeled with Eq. (8); (b) The effect of intra-grain scattering by comparing Eqs. (8) and (10). The plots are given as a function of the grain size.

In Fig. 5(a) we have analyzed Eq. (8) by studying the effect of bulk thermal conductivity on the thermal effective conductivity of UNCD materials. We considered two values of bulk crystalline diamond: the measured value of  $2200 \text{ Wm}^{-1}\text{K}^{-1}$  [1, 2] and the calculated value of  $1265 \text{ Wm}^{-1}\text{K}^{-1}$  [12]. The value of Kapitza resistance was a typical one of  $R_K = 0.15 \times 10^{-9} \text{ Km}^2/\text{W}$ . We can easily notice that for grain sizes up to 100 nm the effective thermal conductivity is insensitive to the thermal conductivity of the crystalline bulk diamond. This is valid as long as  $R_K \kappa_1 / l \gg 1$  according to Eq. (8).

In Fig. 5(b) we compare the effect of intra-grain conductivity/scattering on the effective conductivity of NCD and UNCD materials by comparing Eq. (10), where intra-grain scatterings are considered, with Eq. (8), where such effects are neglected. We notice that the curves have similar shapes. Nevertheless, intra-grain scatterings lower the effective conductivity of poly-

crystalline diamond for the whole range of crystallite sizes from 2 nm to 10  $\mu\text{m}$ .

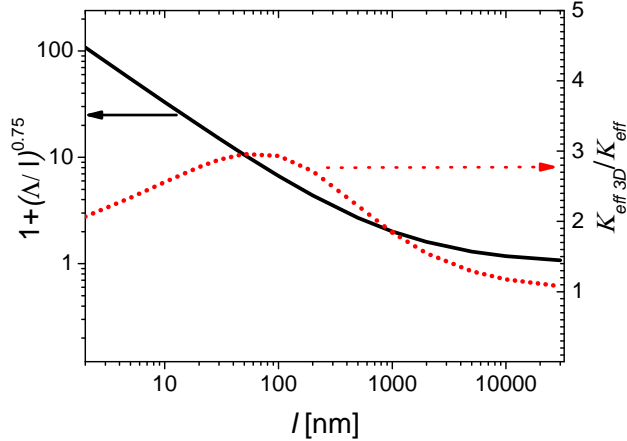


Figure 6: The grain-size dependence of the term  $(1 + \Lambda/l^{0.75})$  responsible for the intra-grain scattering on the left-hand side  $y$ -axis of the graph (solid black line). On the right-hand side  $y$ -axis of the graph is illustrated the ratio  $\kappa_{eff 3D}/\kappa_{eff}$  (dotted red line). The arrows show the assignment of curves with their corresponding  $y$ -axis.

To gain more insight into the effect of intra-grain scattering we also plotted the term  $(1 + \Lambda/l^{0.75})$  as a function of  $l$  with the  $y$ -axis on the left-hand side of Fig. 6. It can be seen that the term varies strongly by almost a factor of 100 for grain sizes ranging from 2 nm to 10  $\mu\text{m}$ , yet this variation cannot be found in the effective conductivities shown in Fig. 5(b). On the  $y$ -axis of the right-hand side of Fig. 6 we plotted the ratio  $\kappa_{eff 3D}/\kappa_{eff}$ . The term  $\kappa_{eff}$  is given by Eq. (10) and  $\kappa_{eff 3D}$  is that of Eq. (8). The ratio is between 2 and 3 for a quite extended range of grain sizes (i. e., from 2 nm to almost 1  $\mu\text{m}$ ) with its peak value at 100 nm and it reaches a value close to 1 for grain sizes of 10  $\mu\text{m}$ . Thus, for small grains, even though the intra-grain scattering is quite large, the intra-grain phonon mean free path lowers the effective conductivity only by a factor of at most 1/3 due to the role played by Kapitza resistance. The role of intra-grain conductivity, which is given by intra-grain scattering, was also analyzed recently in [21], where it was noticed a large discrepancy of Kapitza resistance between the value obtained from the fit of experimental data to Eq. (8) and the results of Kapitza resistance extracted from molecular dynamics simulations [22]. In principles, Kapitza

resistance would also vary with the grain size. Using planar geometries the intra-grain conductivity as well as Kapitza resistance were estimated from molecular dynamics in [21]. As a general trend it was found that Kapitza resistance increases with grain size. This trend of increasing thermal boundary resistance with grain size is also found by analyzing the experimental data from Refs [9, 23], however this increase is offset by the geometrical factor  $l$ .

#### 4. Conclusions

In this work we have studied the effective thermal conductivity of both nanocrystalline and ultra-nanocrystalline diamond films by EMT approaches. Usually the EMT models invoke the approximation of spherical-shaped inclusions. These models are extensively used with good results, but they are inconsistent with respect to polycrystalline films because the maximal packing with spheres is 74%. We formulate an EMT model that can handle in principles any shape of the inclusions. Within this model we compare an EMT model based on spherical inclusions with an EMT model based on cubic inclusions. The results of these two models are very similar. In the following we provide a geometrical argument based on the spectral properties of the electrostatic operator for sphere and cube [14, 18, 20]. Thus we invoke Eq. (7) and the following sum rules [15, 18]:  $\sum_k w_k = 1$  and  $\sum_k w_k L_k = 1/6$ , as well as the inequality  $0 < L_k < 1$ . For large crystallite sizes,  $R_K \kappa_1 / l \ll 1$ , thus the effective conductivity approaches the bulk value regardless of the crystallite shape. On the contrary, for nanometer sized crystallites,  $R_K \kappa_1 / l \gg 1$ , the effective conductivity is  $\kappa_{eff} \approx \sum_k w_k l / (d R_K L_k)$ . Knowing that  $|1 - 2L_k| < 1$  and looking at the spectral parameters  $\{w_k, L_k\}$  of both sphere and cube, we may perform the following approximations

$$\sum_k w_k / L_k = \sum_k \frac{2w_k}{1 - (1 - 2L_k)} \approx \sum_k 2w_k (1 + (1 - 2L_k)).$$

Finally, using the sum rules shown above we conclude that the EMT model based on spherical inclusions gives similar results with the model based on cubic inclusions. We further notice that both types of inclusions (spherical and cubical) preserve macroscopic thermal isotropy of a polycrystalline film.

Moreover, we have found that for grain sizes below 100 nm the effective conductivity is strongly affected by both the boundary Kapitza resistance and

the intra-grain scattering, both of them increasing with grain size. However, the increase of Kapitza resistance is offset by the geometrical effect of the grain size.

## References

- [1] A. L. Moore, L. Shi, Emerging challenges and materials for thermal management of electronics, *Materials Today* 17 (2014) 163–714.
- [2] O. Williams, Nanocrystalline diamond, *Diam. Relat. Mater.* 20 (2011) 621–640.
- [3] O. A. Shenderova, D. M. Gruen, *Ultrananocrystalline Diamond: Synthesis, Properties, and Applications*, William Andre, Norwich, NY, 2006, Ch. 3.
- [4] C. W. Nan, R. Birringer, Determining the Kapitza resistance and the thermal conductivity of polycrystals: A simple model, *Phys. Rev. B* 57 (1998) 8264.
- [5] Z. Wang, J. E. Alaniz, W. Jang, J. E. Garay, C. Dames, Thermal conductivity of nanocrystalline silicon: Importance of grain size and frequency-dependent mean free paths, *Nano Lett.* 11 (2011) 2206–2213.
- [6] Y. Xu, G. Li, Strain effect analysis on phonon thermal conductivity of two-dimensional nanocomposites, *J. Appl. Phys.* 106 (2009) 114302.
- [7] Q. Hao, G. Zhu, G. Joshi, X. Wang, A. Minnich, Z. Ren, G. Chen, Theoretical studies on the thermoelectric figure of merit of nanograined bulk silicon, *Appl. Phys. Lett.* 97 (2010) 063109.
- [8] L. Braginsky, V. Shklover, H. Hofmann, P. Bowen, High-temperature thermal conductivity of porous  $\text{Al}_2\text{O}_3$  nanostructures, *Phys. Rev. B* 70 (2004) 134201.
- [9] M. Shamsa, S. Ghosh, I. Calizo, V. Ralchenko, A. Popovich, A. A. Balandin, Thermal conductivity of nitrogenated ultrananocrystalline diamond films on silicon, *J. Appl. Phys.* 103 (2008) 083538.
- [10] H. S. Yang, G. R. Bai, L. Thompson, J. Eastman, Interfacial thermal resistance in nanocrystalline yttria-stabilized zirconia, *Acta Mater.* 50 (2002) 2309–2317.

- [11] J. Sermeus, B. Verstraetena, R. Salenbiena, P. Pobedinskas, K. Haenen, C. Glorieux, Determination of elastic and thermal properties of a thin nanocrystalline diamond coating using all-optical methods, *Thin Solid Films* 590 (2015) 284292.
- [12] H. Dong, B. Wen, R. Melnik, Relative importance of grain boundaries and size effects in thermal conductivity of nanocrystalline materials, *Sci. Rep.* 4 (2014) 7037.
- [13] T. Sandu, M. Gologanu, R. Voicu, G. Boldeiu, V. Moagar-Poladian, Modeling issues regarding thermal conductivity of graphene-based nanocomposites, *ROMJIST* 21 (2018) 82–92.
- [14] C. W. Nan, Physics of inhomogeneous inorganic materials, *Prog. Mater. Sci.* 37 (1993) 1–116.
- [15] T. Sandu, D. Vrinceanu, E. Gheorghiu, Linear dielectric response of clustered living cells, *Phys. Rev. E* 81 (2010) 021913.
- [16] G. E. Gubernatis, Scattering theory and effective medium approximations to heterogeneous materials, in: *American Institute of Physics Conference Series*, Vol. 40 of American Institute of Physics Conference Series, 1978, pp. 84–98.
- [17] C. W. Nan, R. Birringer, D. R. Clarke, H. Gleiter, Effective thermal conductivity of particulate composites with interfacial thermal resistance, *J. Appl. Phys.* 81 (1997) 6692–6699.
- [18] R. S. Koss, D. Stroud, Applications of the effective-medium approximation to cubic geometries, *Phys. Rev. B* 32 (1985) 3456–3461.
- [19] A. Bejan, A. D. Kraus, *Heat transfer handbook*, 2nd Edition, John Wiley & Sons, New York, NY, 2003.
- [20] R. C. Voicu, T. Sandu, Analytical results regarding electrostatic resonances of surface phonon/plasmon polaritons: separation of variables with a twist, *Proc. R. Soc. A* 473 (2017) 2016079.
- [21] D. Spiteri, J. Anaya, M. Kuball, The effects of grain size and grain boundary characteristics on the thermal conductivity of nanocrystalline diamond, *J. Appl. Phys.* 119 (2016) 085102.

- [22] M. A. Angadi, T. Watanabe, A. Bodapati, X. Xiao, O. Auciello, J. A. Carlisle, J. A. Eastman, P. Koblinski, P. K. Schelling, S. R. Phillpot, Thermal transport and grain boundary conductance in ultrananocrystalline diamond thin films, *J. Appl. Phys.* 99 (2006) 114301.
- [23] M. Mohr, K. Bruhne, H. J. Fecht, Thermal conductivity of nanocrystalline diamond films grown by hot filament chemical vapor deposition, *physica status solidi (a)* 213 (2016) 2590.